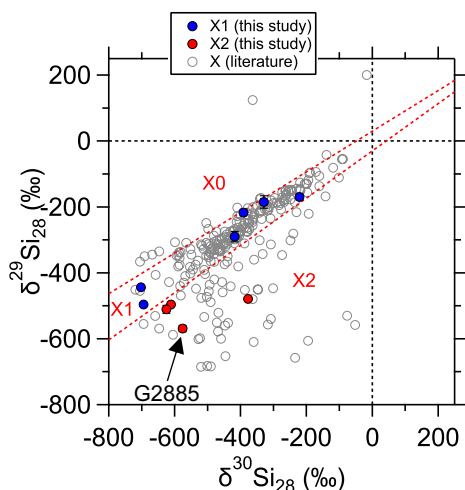


**LATE FORMATION OF SILICON CARBIDE IN SUPERNOVA REMNANTS CONFIRMED BY NEW VANADIUM-TITANIUM ISOTOPE DATA.** N. Liu<sup>1</sup>, C. M. O'D. Alexander<sup>2</sup>, L. R. Nittler<sup>3</sup>, J. Wang<sup>2</sup>, <sup>1</sup>Institute for Astrophysical Research, Boston University, Boston, MA 02215, USA, [nanliu@bu.edu](mailto:nanliu@bu.edu), <sup>2</sup>Earth & Planets Laboratory, Carnegie Institution for Science, Washington, DC 20015, USA, <sup>3</sup>School of Earth and Space Exploration, Arizona State University, Tempe, AZ, 85287, USA.

**Introduction:** The contribution of core-collapse supernovae (CCSNe) to the cosmic dust reservoir in the Universe is highly debated. While the large amounts of dust observed for young galaxies suggest production of  $\geq 0.1 M_{\odot}$  dust per CCSN, e.g., [1], theoretical models predict that the initially formed dust is efficiently (up to 100%) destroyed later by the reverse supernova shock, e.g., [2]. Observations of dust formation timing and production quantity in CCSNe are thus required to directly evaluate the role of CCSNe in contributing to the cosmic dust reservoir over time.



**Fig. 1.** Si 3-isotope plot. The subtype classification scheme for X grains was introduced in [3].

Presolar X SiC grains, which are divided into three subtypes based on Si isotopes (Fig. 1), are inferred to have come from ancient CCSNe [4]. Radiometric dating of X grains provides us a unique opportunity to constrain dust formation timing in ancient CCSNe. Based on the  $^{49}\text{V}$ - $^{49}\text{Ti}$  ( $t_{1/2} = 330$  d) systematics, Liu et al. [5] concluded that X grains formed at least two years after the explosion of their parent CCSNe. This result is in line with the conclusion of Ott et al. [6] ( $\sim 20$  a) based on the  $^{137}\text{Cs}$ - $^{137}\text{Ba}$  ( $t_{1/2} = 30$  a) systematics, both of which consistently point to late formation of CCSN dust. Stephan et al. [7],

however, suggested that X2 grains formed earlier ( $< 1$  a) based on Sr and Ba isotopes, raising the possibility of varying dust formation conditions among CCSNe. Here, we report V-Ti isotope data for 10 new X grains to (i) better constrain the dust formation timing by improving the statistics, and (ii) further investigate whether X1 and X2 grains formed at different times.

**Experimental Methods:** The SiC grains in this study were extracted from Murchison (CM2) using the CsF dissolution technique described in [8]. A total of 450 SiC grains were measured for their C, N, and Si isotopes, based on which 22 X grains were identified. The X grains were further analyzed for their V-Ti and Al-Mg isotopes with the Carnegie NanoSIMS 50L ion microprobe following the procedures reported in [5]. An  $\text{O}^-$  beam of 1–3 pA produced by the Hyperion radio-frequency plasma source was used for analysis. All the isotope data were collected in imaging mode at a spatial resolution of  $\sim 100$ – $200$  nm (Fig. 2).

**Results:** Aluminum-Mg isotope data were obtained for all the 22 X grains and are reported separately in [9]. Also, V-Ti isotope data were obtained for 10 of the 22 X grains that had relatively high Ti and low Ca and Cr contents, i.e., no significant isobaric interferences. Figure 2 illustrates that the improved ion image spatial resolution in this study enabled suppressing (i) isobaric interferences at mass 50 (from  $^{50}\text{Cr}$ ), and (ii) sampling extrinsic signals from adjacent grains by choosing smaller regions of interest for data reduction.

The Ti isotopic compositions of all but one X grain are characterized by close-to-solar  $\delta^{46}\text{Ti}_{48}$  and  $\delta^{47}\text{Ti}_{48}$  values and large  $^{49}\text{Ti}$  excesses (up to 1200‰), consistent with previous findings, e.g., [5]. The one exception is an X2 grain (G2885 in Fig. 1) that has a composition of  $\delta^{46}\text{Ti}_{48} = -476 \pm 64\%$ ,  $\delta^{47}\text{Ti}_{48} = -288 \pm 64\%$ ,  $\delta^{49}\text{Ti}_{48} = 95 \pm 68\%$ , and  $\delta^{50}\text{Ti}_{48} = -212 \pm 58\%$  ( $1\sigma$  errors), pointing to its larger  $^{48}\text{Ti}$  excess as compared to the other X grains.

**Discussion:** That most X grains fall along a line in Fig. 1 points to two-endmember mixing, which suggests that X grains sampled materials mainly from the inner

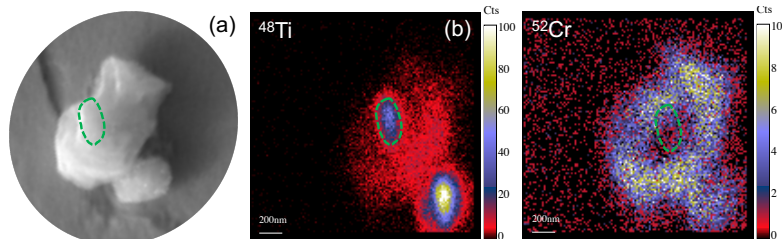


**Fig. 2.** Secondary electron (panel a) and NanoSIMS ion images (panels b and c) of an X grain that sits next to a smaller Ti-rich mainstream SiC grain. The green contour line highlights a Ti-rich subgrain within the X grain.

Si/S zone that is almost purely enriched in  $^{28}\text{Si}$  and the outer C-rich zones, i.e., the He/C zone and zones above it (hereafter outer zones), that are relatively more enriched in  $^{29}\text{Si}$  and  $^{30}\text{Si}$  [4]. Like Si isotopes, almost pure  $^{48}\text{Ti}$  enrichments are predicted for the inner Si/S zone, and  $^{49}\text{Ti}$  and  $^{50}\text{Ti}$  enrichments for the outer zones. In contrast to Si isotopes, the Ti isotope composition of the Si/S zone changes with time as  $^{49}\text{Ti}$  increases because of radiogenic decay of  $^{49}\text{V}$  ( $t_{1/2} = 330$  d).

Given the facts above, Liu et al. [5] developed a method to calculate the  $\delta^{49}\text{Ti}$  value in the Si/S zone at the time of SiC dust formation, as illustrated in Fig. 3. In the figure,  $\delta^{49}\text{Ti}_{48}^*$  denotes  $\delta^{49}\text{Ti}_{48}$  of a grain after subtracting the amount of  $^{49}\text{Ti}$  that is made by neutron capture in the He/C zone (see [5] for details). To do so, one needs to know the neutron-capture production ratio of  $^{49}\text{Ti}/^{50}\text{Ti}$  in the He/C zone. Liu et al. [5] inferred a production ratio of unity based on the Ti isotopic compositions of three ungrouped CCSN grains that sampled more materials from the outer zones. Given the inferred production ratio of unity,  $\delta^{49}\text{Ti}_{48}^*$  can be calculated using the equation  $\delta^{49}\text{Ti}_{48}^* = \delta^{49}\text{Ti}_{48} - \delta^{50}\text{Ti}_{48} - 1000$  (see [5] for the derivation in detail). Since an X grain with  $\delta^{30}\text{Si}_{28} = -1000\text{‰}$  means that the grain incorporated pure Si/S material, the intercept of the fit line at  $\delta^{30}\text{Si}_{28} = -1000\text{‰}$  in Fig. 3 represents the average  $\delta^{49}\text{Ti}_{48}$  in the Si/S zone when the X grains formed in their parent CCSNe.

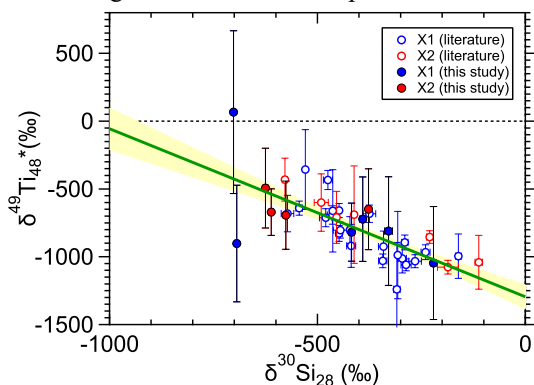


**Fig. 3.** Plot of  $\delta^{49}\text{Ti}_{48}^*$  versus  $\delta^{30}\text{Si}_{28}$ . The negative trend shown as a linear fit line (green solid line) with 95% confidence (yellow band) results from variable contributions from the He/C zone to the grains'  $^{48}\text{Ti}$  and  $^{30}\text{Si}$  budgets. Errors are  $2\sigma$ .

The new X grain data are in good agreement with the literature data within uncertainties. With the increased statistics (40 X grains in total), we still see no difference between X1 (29 in total) and X2 (11 in total) grains in their  $\delta^{49}\text{Ti}_{48}^*$  values, implying that the two subtypes of X grains both formed late so that they received comparable contributions of  $^{49}\text{Ti}$  from  $^{49}\text{V}$  decay.

Four of the 10 X grains from this study have larger  $^{28}\text{Si}$  excesses than those from the literature (Fig. 3), thus

allowing us to constrain the intercept at  $\delta^{30}\text{Si}_{28} = -1000\text{‰}$  more precisely. While Liu et al. [5] constrained the  $\delta^{49}\text{Ti}_{48}$  in the Si/S zone at the time of grain formation to  $282 \pm 305\text{‰}$ , the enlarged new dataset revises the constraint to  $-56 \pm 150\text{‰}$ , yielding an average formation timing of  $1.8 \pm 0.7$  years after the explosion of their parent CCSNe. However, since the Ti/Si elemental ratio is much higher in the Si/S zone than in the outer zones, the mixing line in Fig. 3 is expected to have curvatures with increasingly steepened slopes toward  $\delta^{30}\text{Si}_{28} = -1000\text{‰}$ , which would lead to larger  $\delta^{49}\text{Ti}_{48}^*$  at  $\delta^{30}\text{Si}_{28} = -1000\text{‰}$  than the extrapolated value based on the linear fit in Fig. 3. Consequently, this means that SiC dust is more likely to have formed later than 1.8 years and that our derived upper limit (2.5 years) is underestimated. More sophisticated calculations incorporating CCSN models are being investigated.

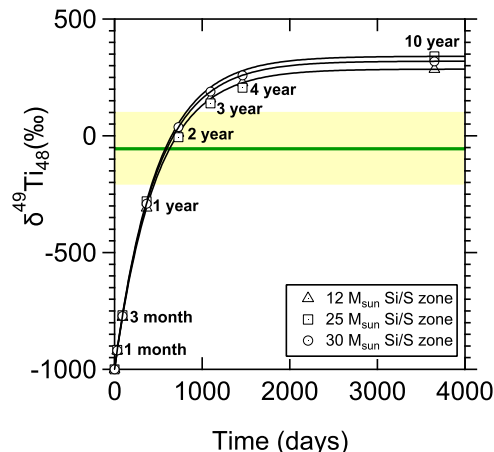


**Fig. 4.** Growth curves of  $\delta^{49}\text{Ti}_{48}$  in the Si/S zone resulting from  $^{49}\text{V}$  decay predicted by the models of [10]. The  $\delta^{49}\text{Ti}_{48}$  value obtained by the linear fit in Fig. 3 is shown (green line) with 95% confidence (yellow band).

**Conclusions:** Our V-Ti isotope data for 10 new X grains provided further evidence to support the late formation of dust in supernova remnants, in line with recent astronomical observations [11]. Our new data also indicate that there is no systematic difference in the formation timing between X1 and X2 grains, implying similar dust formation conditions among CCSNe.

**References:** [1] Laporte N. et al. (2017) *A&A* **837**, L21. [2] Slavin J. D. et al. (2020) *ApJ* **902**, 135. [3] Lin Y. et al. (2010) *ApJ* **709**, 1157–1173. [4] Nittler L. R. et al. (1996) *ApJ* **462**, L31. [5] Liu N. et al. (2018) *Sci. Adv.* **4**, aao1054. [6] Ott U. et al. (2019) *ApJ* **885**, 128. [7] Stephan T. et al. (2018) *GCA* **221**, 109–126. [8] Nittler L. R. & Alexander C. M. O'D. (2003) *GCA* **67**, 4961–4980. [9] Liu N. et al. (2023) *54<sup>th</sup> LPSC*, this volume. [10] Woosley S. E. & Heger A. (2007) *Phys. Rep.* **442**, 269–283. [11] Niculescu-Duvaz M. et al. (2022) *MNRAS* **515**, 4302–4343.